SAND2017-6307C

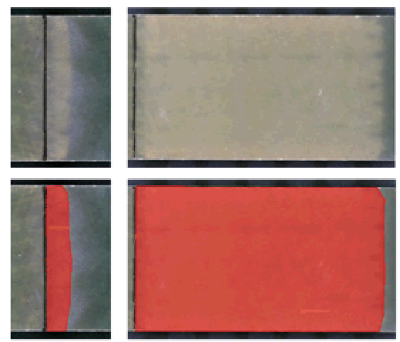

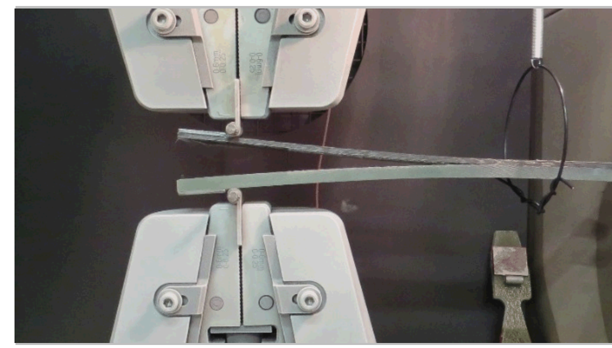

Effect of Process Induced Stresses on Measurement of FRP Strain Energy Release Rates

Brian Werner, Stacy M. Nelson, Timothy M. Briggs

Sandia National Laboratories, Livermore, CA

SEM Annual 2017 Conference and Exposition on Experimental and Applied Mechanics

Indianapolis, IN June 12-15, 2017

Motivation

- High fidelity computer simulations can be used to promote better understanding of experimentally observed behaviors
- Composites are frequently used in hybrid structures that bond dissimilar materials and introduce significant residual stresses
- Residual stresses have been observed to increase the apparent fracture toughness
- Possible explanations for this behavior have been hypothesized:
  - CTE mismatch between composite adherends leads to an increase in mode-mixity that promotes high toughnesses
  - Thermal contractions within the bondline after an elevated temperature cure causes compression that must be overcome
- The effects of individual phenomena are difficult to determine experimentally

Material

- CFRP
  - AS4/UF3362-100
  - 8-harness satin weave
- GFRP
  - E-glass/UF3362-100
  - 8-harness satin weave
- Co-cured in one step cure
- Layups
  - CFRP/CFRP $[0/90]_{5s}$
  - GFRP/GFRP $[0/90]_{7s}$
  - GFRP/CFRP $[(0/90)_{10s}{}^{G}/(0/90)_{5s}{}^{C}]$
  - Adherends balanced for equal bending stiffness

	CFRP	GFRP
E_{11} (GPa)	63.9	24.8
E_{22} (GPa)	62.7	23.1
E_{33} (GPa)	8.6	9.7
G_{12} (GPa)	3.44	3.4
G_{13} (GPa)	3.27	2.9
G_{23} (GPa)	3.25	2.9
v_{12}	0.048	0.13
v_{13}	0.408	0.36
v_{23}	0.408	0.36
CTE_{11} (rubbery) (ppm/ºC)	1.14	8.31
CTE_{22} (rubbery) (ppm/ºC)	1.36	9.88
CTE_{33} (rubbery) (ppm/ºC)	282.9	343.5
CTE_{11} (glassy) (ppm/ºC)	3.41	17.3
CTE_{22} (glassy) (ppm/ºC)	3.42	17.9
CTE_{33} (glassy) (ppm/ºC)	72	65.6
T_g (ºC)	122.7	104.5
Stress-Free Temperature (ºC)	140	140

Experimental Procedure

- Tests were completed in accordance with ASTM test standard D5528 and D7905
- Experiments utilized an Instron 5989 electromechanical load frame with a 2kN load cell
- Specimens tested with constant displacement rate of 1 mm/min
- Load and crosshead displacement data were recorded during each test
- Tests were completed at three test temperatures:
  - -54° C, 25° C, 71° C
- Crack length and mode I fracture toughness were calculated with the recorded data

$$a = \left[\frac{\delta b}{16P}\left(E_1 h_1^3 + E_2 h_2^3\right)\right]^{\frac{1}{3}}$$

$$G_{app} = \left[\frac{27\delta^2}{2b^4}\left(\frac{1}{E_1 h_1^3} + \frac{1}{E_2 h_2^3}\right)P^4\right]^{\frac{1}{3}}$$

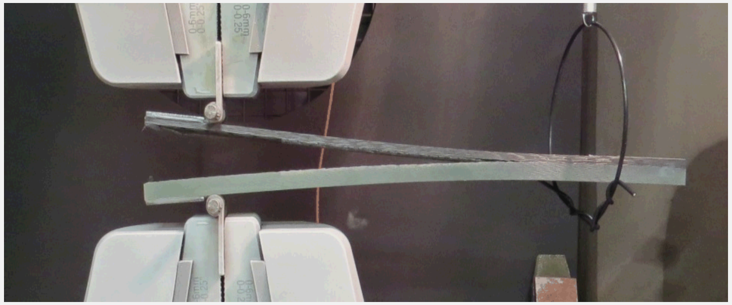

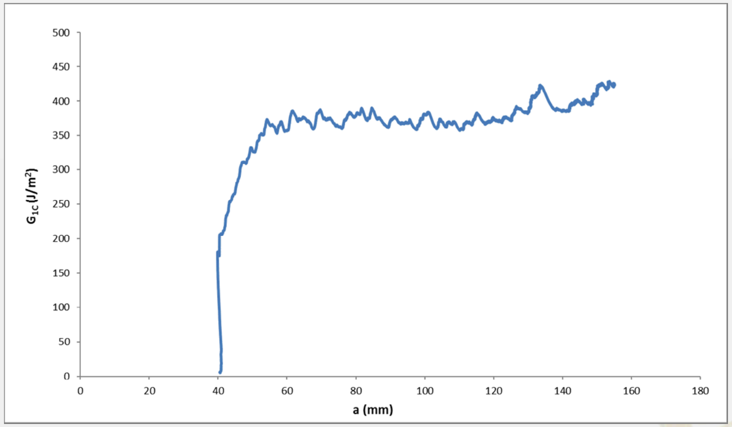

DCB Testing – Bulk Material

- Bulk material fracture toughness shows no temperature dependence
- GFRP-GFRP specimens fail at the matrix-to-fiber interface
  - SEM of glass fiber to resin failure
  - 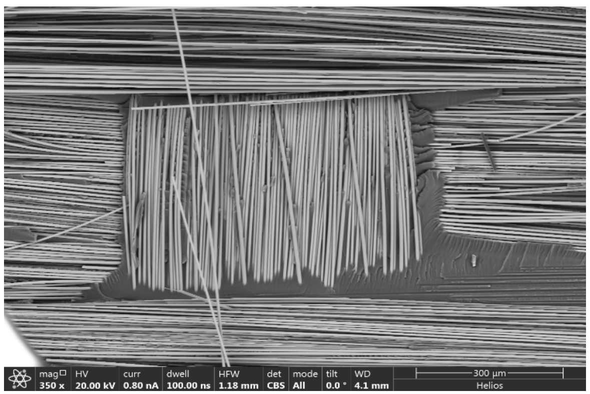

- CFRP-CFRP specimens exhibit more unstable crack growth potentially due to larger fiber bundles resulting in a coarser weave

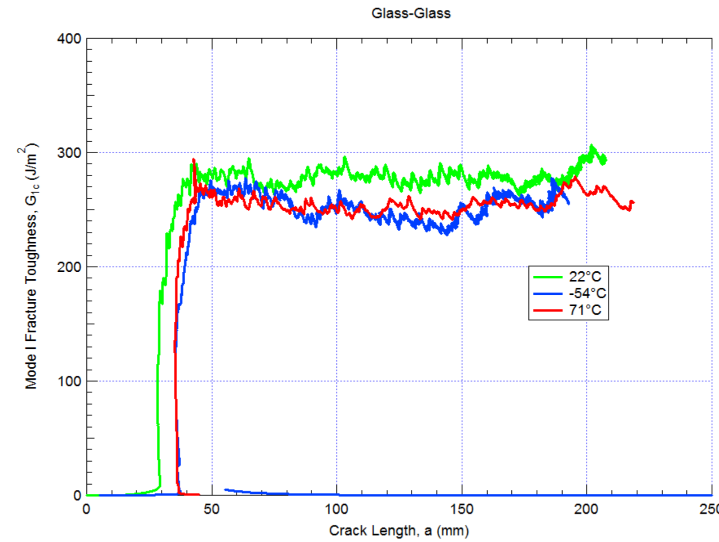

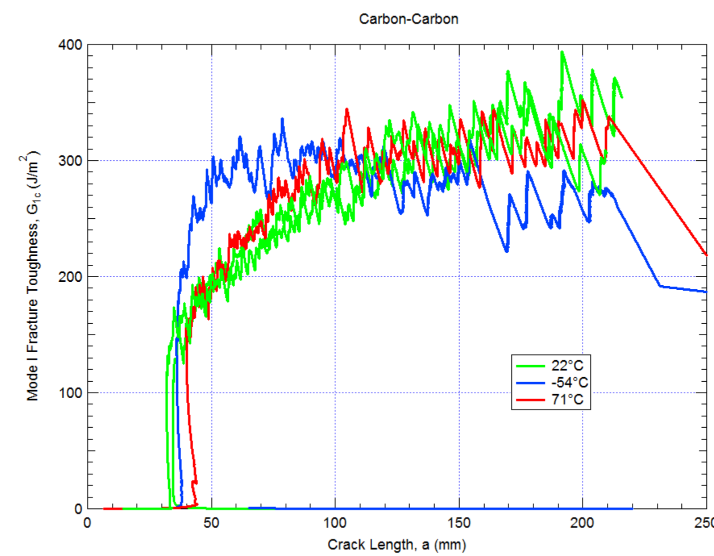

DCB Testing – Bi-Material

- CFRP-GFRP fracture toughness shows significant temperature dependence
  - Residual stress, failure mode
- Room and sub-ambient temperature tests show some rising resistance
  - 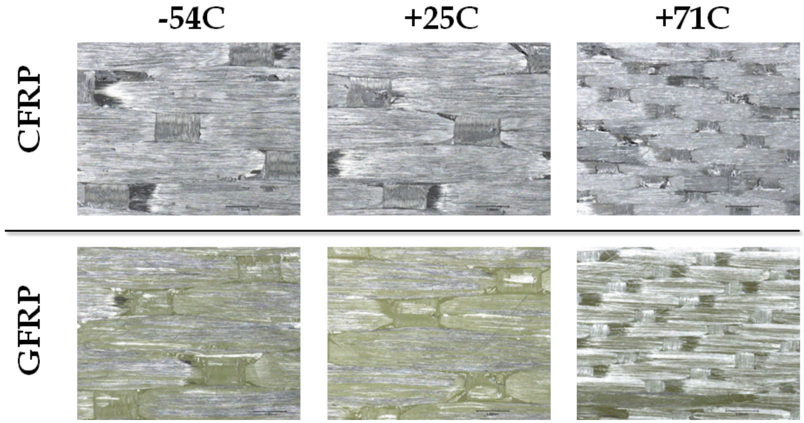

- Fracture toughness increases with decreasing temperature suggests residual stress provides favorable stress state

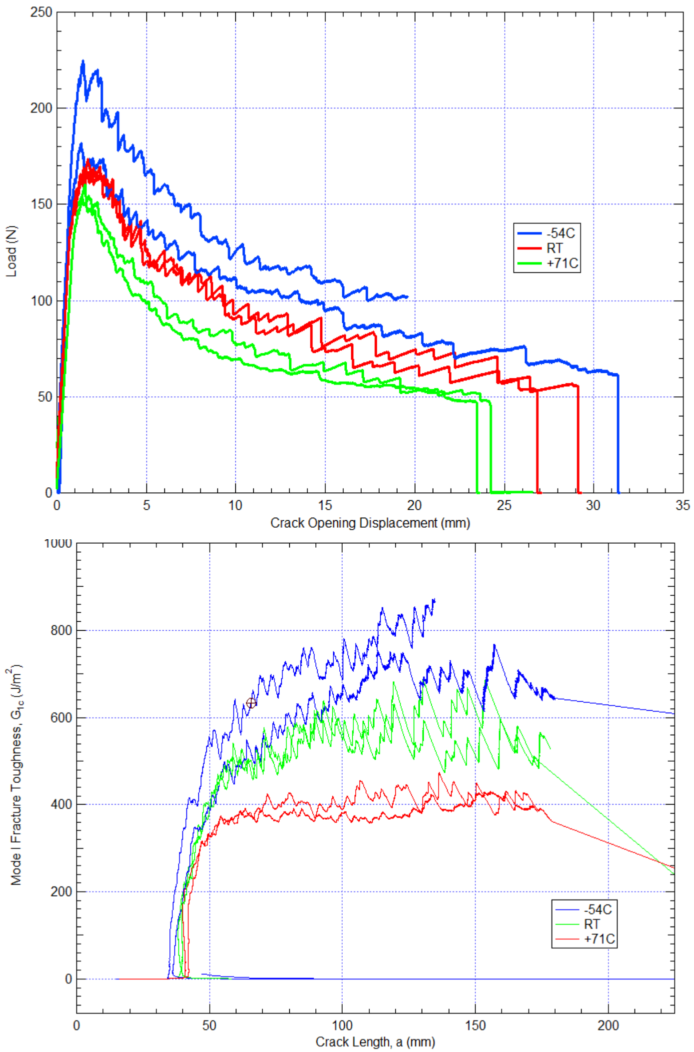

ENF Testing

- Performed in accordance with ASTM D7905
- Standard is for UD composites but adapted here for woven composites
- Displacement measured with a laser extensometer
- Balance found between stable and unstable crack growth in specimen design

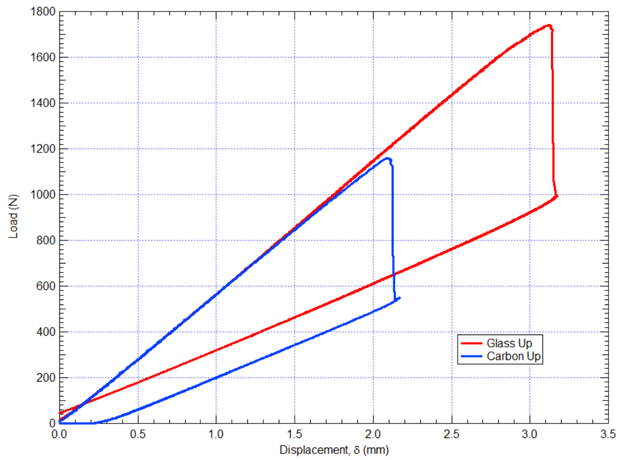

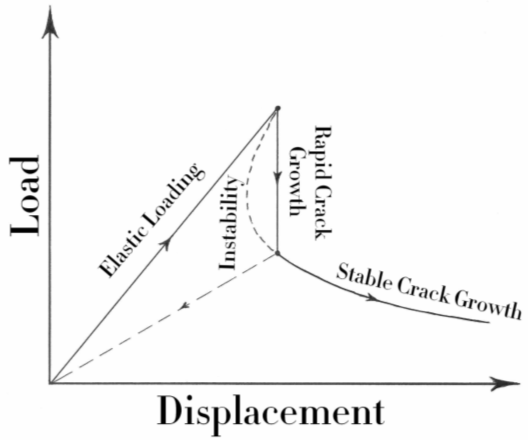

Sketch courtesy of Joel Fenner, Northwestern University

ENF Geometry

- Difficult to find guidelines on correct specimen geometry
- Longer crack length produces stable crack growth but more frictional losses and less new surface area produced
- Span and initial crack length varied and repeatability compared (3 specimens each)
- Span of 2L varied: 4”, 5”, 6”
- Initial crack length varied: 0.3L, 0.5L, 0.69L
- All tests performed with glass facing up
- Longest span and middle average crack length chosen for study

Span (2L)	Crack Length	G Avg (J/m^2)	COV (%)
102mm	0.3L	2636	16.1
	0.5L	1434	5.0
	0.69L	1308	18.6
127mm	0.3L	2532	15.1
	0.5L	1575	8.8
	0.69L	1319	25.2
152mm	0.3L	3082	5.4
	0.5L	1282	1.6
	0.69L	1273	3.7

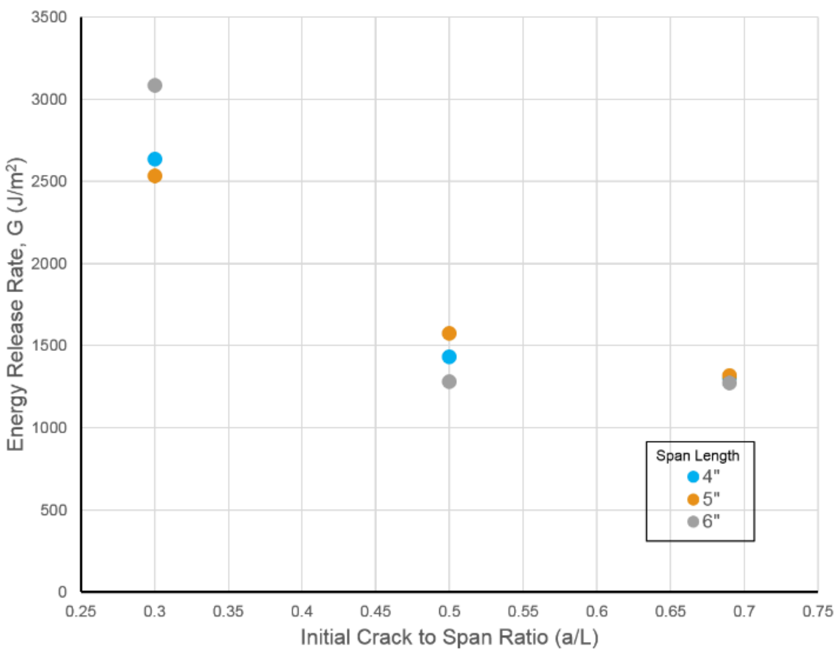

Overhang

- Following specimen geometry study, precracked overhang was investigated
- While not controlled initially, trend appears to show a longer overhang results in larger energy release rate measurements
- For future tests overhang was kept to a minimum

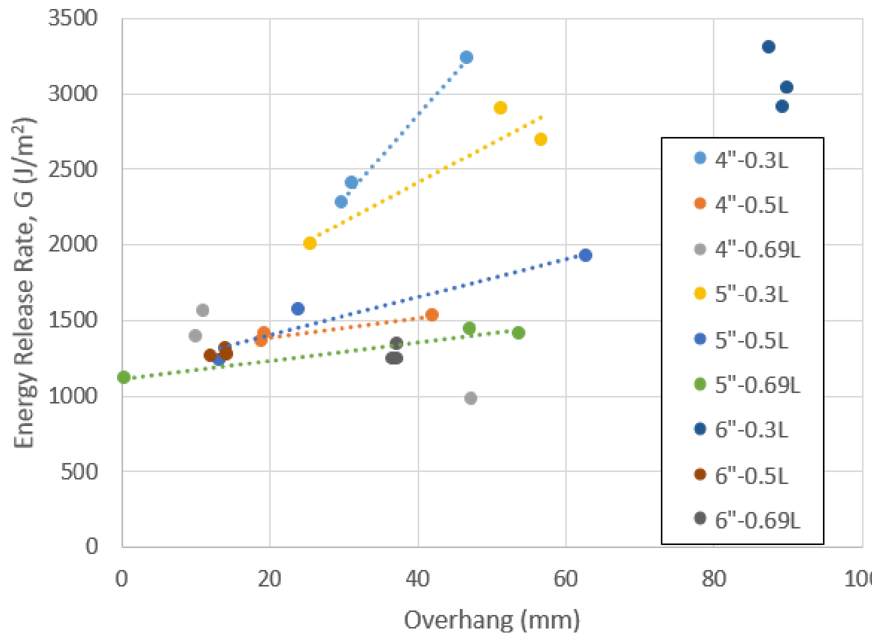

ENF Results

- Subambient tests
  - While the elevated and room temperature tests show a similar trend, the subambient tests displayed much higher energy release rates than anticipated
  - This is due to the tendency of the crack to jump plies and form additional surface area not accounted for in visual measurements
  - Ultrasonics needed to fully characterize new surface area
- Bulk material
  - Consistent results
  - Not much temperature dependence
- Bi-material
  - Diverging trends with increasing residual stress
  - Higher stress reduces *G* for carbon up and increases it for glass up configurations

Specimen Type	Temperature	Face Up	G_{Avg} (J/m^2)	COV (%)
GFRP	71°C	N/A	1230	2.1
	20°C		1172	0.6
	-54°C		1856	5.6
Bi-Material	71°C	Carbon	869	5.7
		Glass	1224	5.6
	20°C	Carbon	733	2.9
		Glass	1281	1.6
	-54°C	Carbon	882	4.9
		Glass	1889	2.1

Residual Stress Modeling with SIERRA/SM

- Residual stress development
  - ***CTE mismatch***
    - CTEs for glassy and rubbery regions are differentiated
  - ***Polymer Shrinkage***
    - "Cure" temperature is the experimentally determined stress free temperature
- ***Constant mechanical properties*** do not vary with temperature
- ***Isothermal specification*** of the thermal cycle
  - No heat transfer analysis done (temperature soak is irrelevant)
- ***Instantaneous change from a uncured to cured*** state at stress free temperature
  - Compliant elements representing uncured composite are deactivated
  - Elements defined with composite's material properties are activated with zero stress

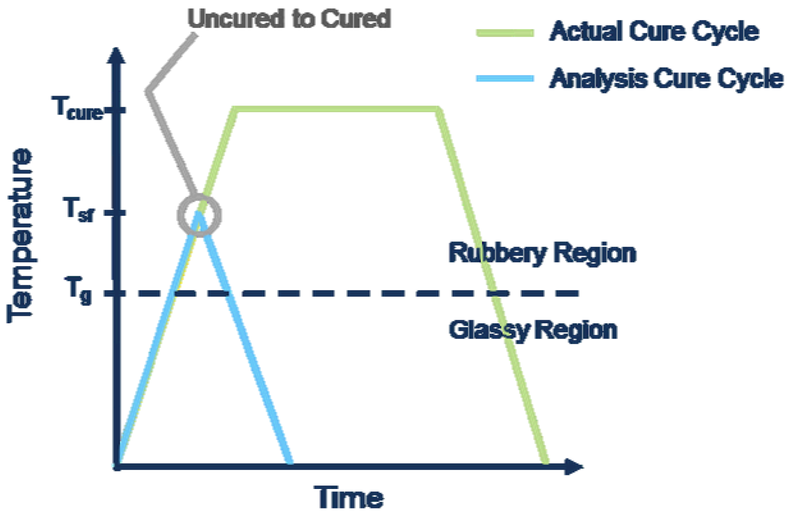

DCB Modeling

- Interface modeling
  - Cohesive surface elements used
  - Zero volume
  - Computationally efficient
- Common approach for modeling delaminations
- Depends on traction-separation law
  - Area under curve is equal to critical energy release rate, G_c
  - Strength/failure separation can be varied
  - Shape not as important as G_c if LEFM holds
  - Bulk material G_c *used*

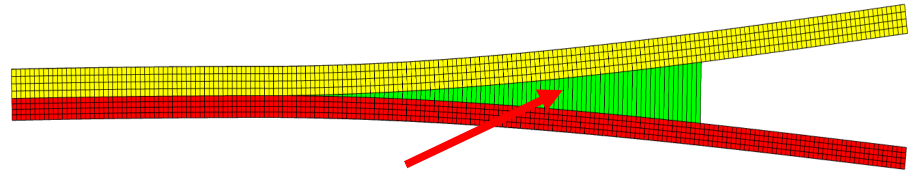

Cohesive zone elements expand to indicate separation governed by traction-separation law

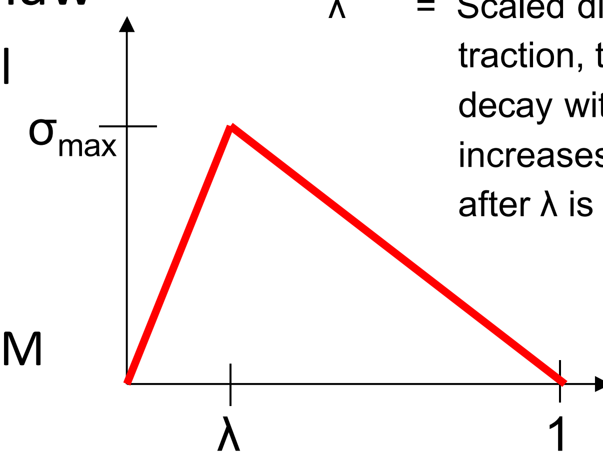

σ_{max} = Peak traction

λ = Scaled distance to peak traction, traction will decay with additional increases in separation after λ is exceeded

Cohesive Zone Results

- Opposite trend with temperature observed
- Adding mode mixity helps the trend
  - Thouless-Parmigiani
  - Still does not match experiment
- Zero volume elements
  - No out-of-plane thermal effects on interface
  - Adhesives typically fail due to maximum principal strain
- Solid elements used to model bondline

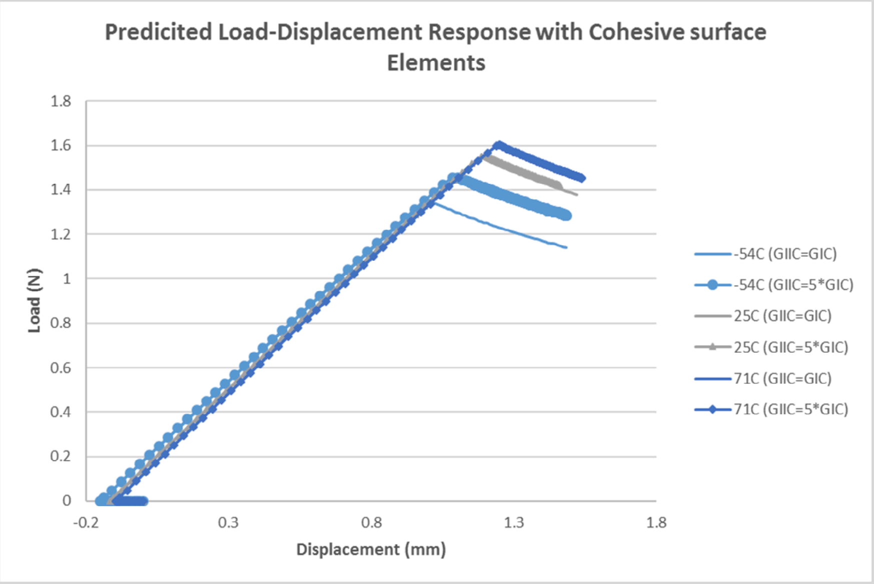

Interface Modeling w/Continuum Elements

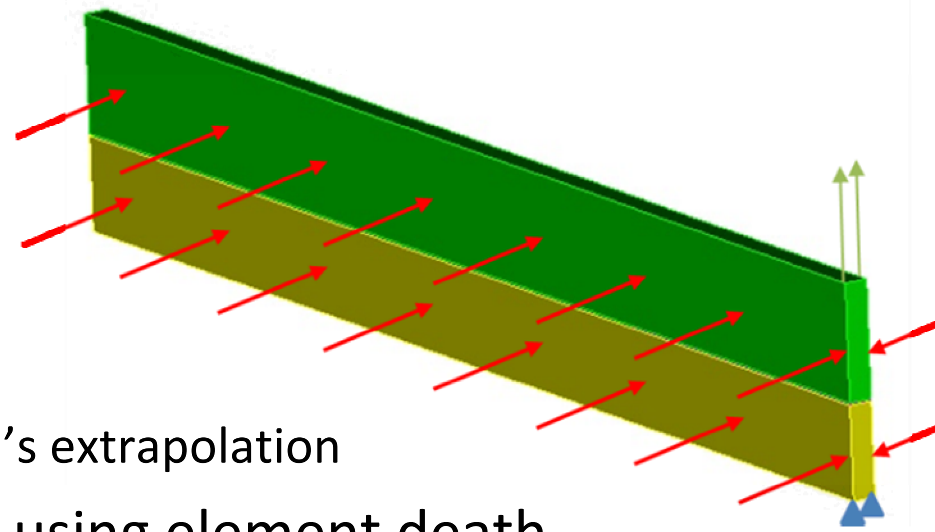

- Plane strain model
- Mesh convergence study
  - Fine mesh chosen
  - 0.04mm element size
  - Negligible error using Richardson's extrapolation
- Crack propagation determined using element death
  - Maximum principal strain failure criterion
  - Mesh dependent – qualitative results

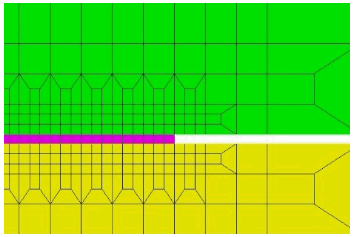

Coarse

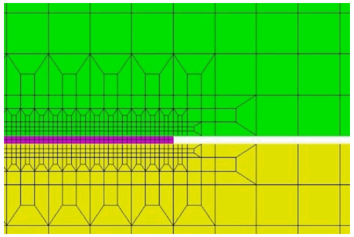

Medium

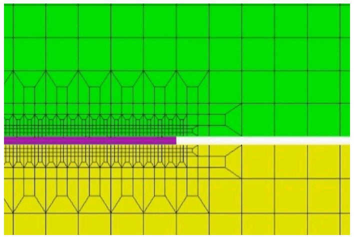

Fine

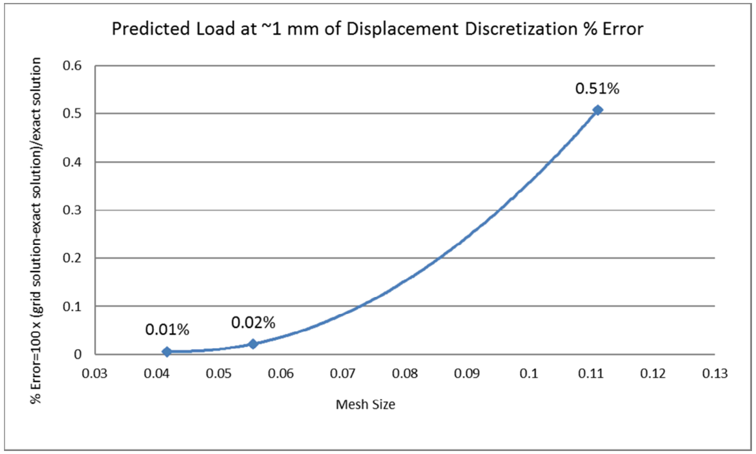

Continuum Results

- Simulations completed with the effect of bondline thermal strains
  - Combined effect of CTE mismatch and bondline contraction
- Simulations match experimental trends
  - Peak loads increase with increasing residual stress levels
  - Slightly higher peak load predictions with bondline contractions
  - Peak load predictions are qualitative only
- Out-of-plane shear/mode II bondline strains are not affected
- Normal/mode I bondline strains are significantly decreased
- Increased peak load predictions are related to higher levels of bondline compression with increasing levels of residual stress

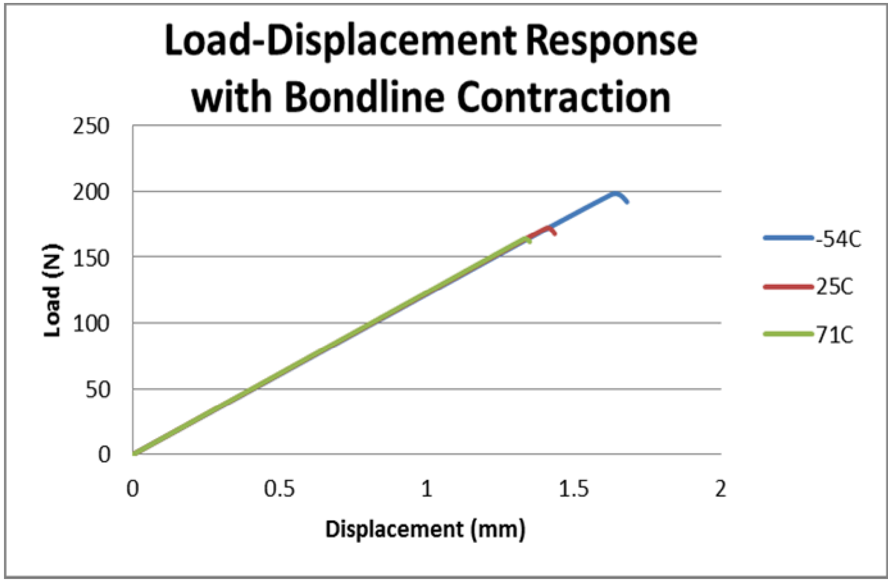

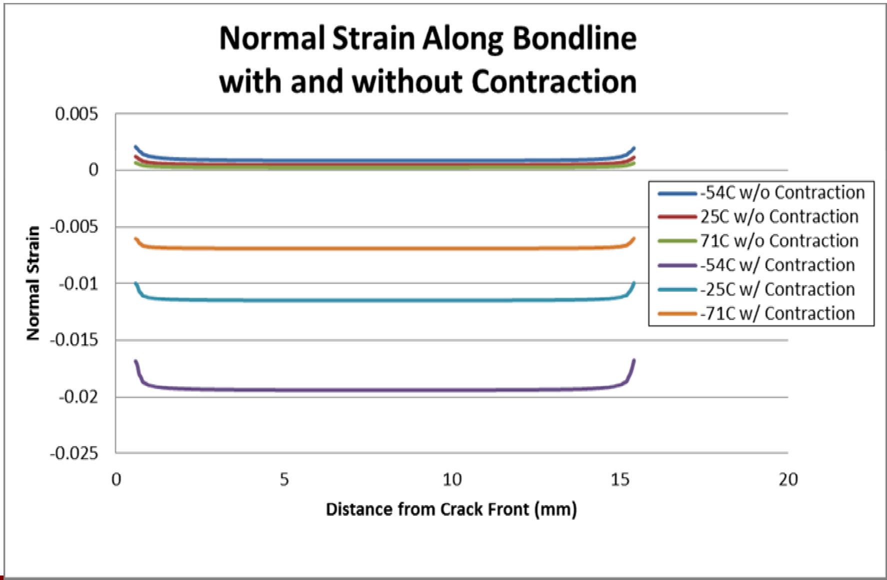

ENF Modeling

- Plane strain model
- Cure cycle simulated
- Specimen cooled until test temperature then loading applied
- Simulations performed with CFRP and GFRP on top
- Solid elements used to model bondline
- Element death determines crack propagation w/maximum principal strain failure criterion

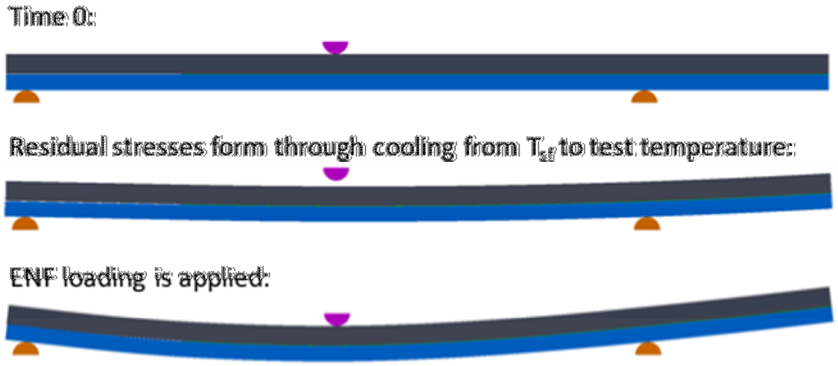

ENF Modeling Results

- Strain field probed at various distances from crack tip
  - Includes residual strains
  - Small elastic mechanical loading applied
- Trends
  - Glass on top
    - High temperature shows largest strains
    - Cold temperature shows smallest
  - Carbon on top
    - Cold temperature shows largest strains
    - High temperature shows smallest
- Residual strains work with mechanical when carbon is on the compression face, against when glass is on the compression face

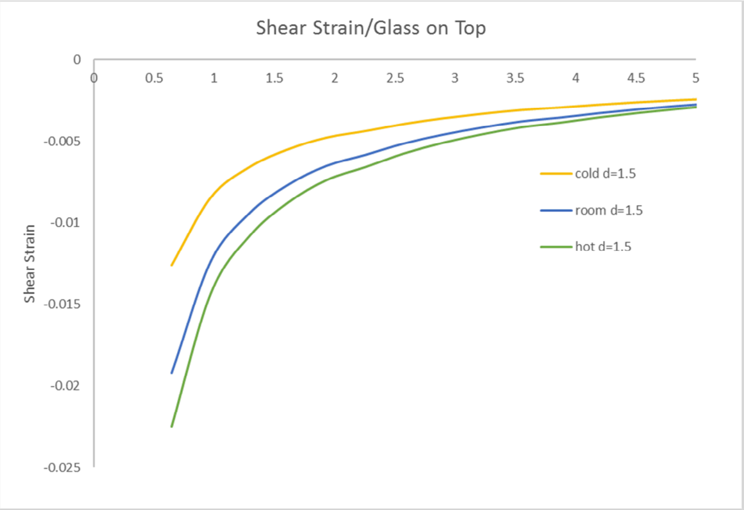

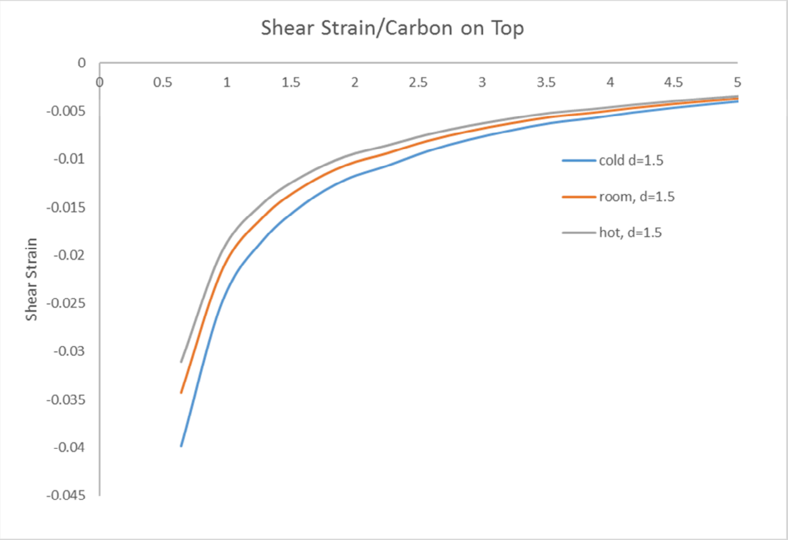

ENF Modeling Results

- Maximum principal failure strain calibrated to experimental results
  - Not predictive for these load cases
  - Demonstration of whether correct trend can be seen
  - Still uses element death
- Qualitative trend does appear to hold
- Aspect of CZ elements does not capture what solid elements can

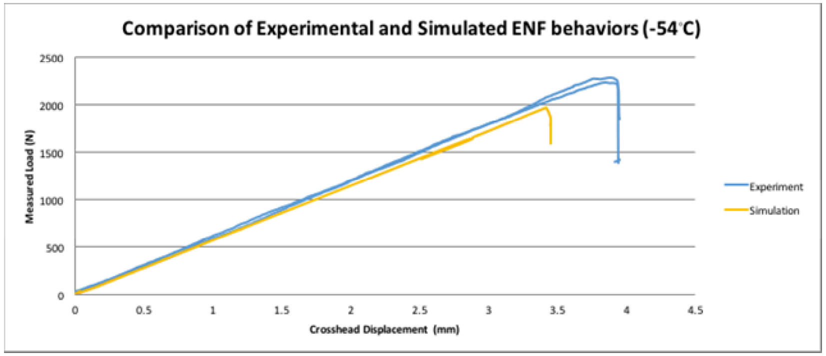

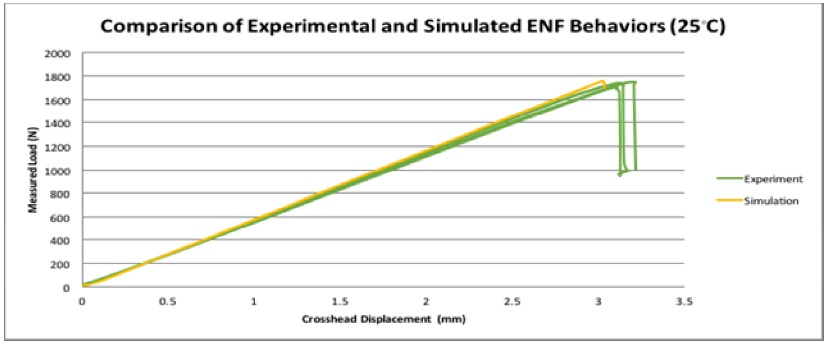

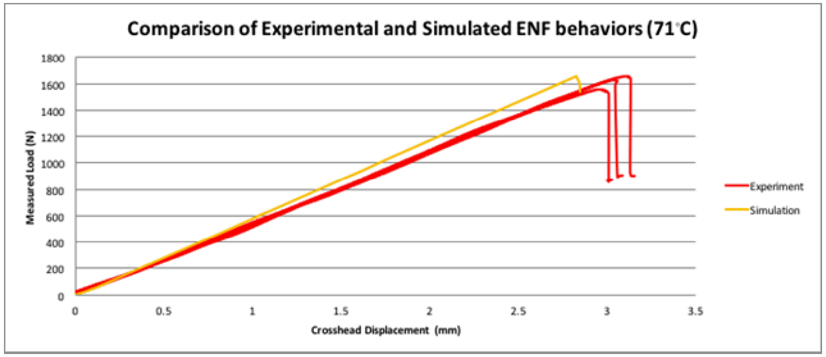

Conclusion

- For ENF testing a precrack length, a, of L/4 produces similar results as stable crack growth when a=0.69L
- Residual stresses can produce swings in apparent critical strain energy release rates
- To use experimental results properly without risking nonconservative designs these effects must be accounted for
- Traditional cohesive zone models may miss the effects of residual stresses
- Open question as to whether residual stresses contribute to a shift in mode-mixity in bi-material interfaces

Future Work

- Mixed mode bending tests at various temperatures to determine if residual stresses contribute to shift in mode-mixity
- Ultrasonic scans of specimens to fully account for increase in crack surface area
- More complex layups to validate resulting interlaminar fracture model